ELSEVIER

Ceramics International 29 (2003) 1–6

CERAMICS INTERNATIONAL

www.elsevier.com/locate/ceramint

Effects of mechanical treatment on phase transformation and sintering of nano-sized γ-Fe_2O_3 powder

Hsing-I Hsiang*, Fu-Su Yen

Department of Mineral and Petroleum Engineering, National Cheng Kung University, Tainan, Taiwan, ROC

Received 14 October 2001; received in revised form 17 November 2001; accepted 19 April 2002

Abstract

The effects of mechanical treatment on the phase transformation and sintering of nano-sized γ-Fe_2O_3 powder were studied. γ-Fe_2O_3 powder was obtained by calcining iron tartrates at 300 °C. The mechanical treatment increased the contact areas in the γ-Fe_2O_3 powder, which acted as nucleation sites for the γ→α-Fe_2O_3 phase transformation, and resulted in lowering the transformation temperature. The greater surface area and fine equiaxed particle of the milled powder thus obtained were due to the vermicular microstructure development being inhibited. Consequently, the samples with mechanical treatment after sintering developed a uniform fine-grained microstructure.

Keywords: A. Sintering; B. Microstructure; Fe_2O_3; Phase transformation; Mechanochemical treatment; Morphology

1. Introduction

Iron oxide is widely used as a catalyst, pigment and gas sensitive material [1]. In many cases nanocrystalline iron oxide can enhance materials performance or improve industrial processing. For instance, synthesis of ferrites can be achieved at a much lower temperature by using nano-sized iron oxide as a raw material [2]. Additionally, the gas sensitivity of α-Fe_2O_3 also can be improved remarkably by using the ultrafine α-Fe_2O_3 powders [3]. Therefore it is of importance to control the particle size, morphology, and texture of the iron oxide system.

Recently, many different methods have been used in preparing nanosized α-Fe_2O_3. Among the various methods, the thermal decomposition of precursors, such as tartrates [4] and ferrous oxalate dihydrate [5] have been widely investigated due to the benefits of easily controlled process and lower cost. There are two well-known crystalline types of Fe_2O_3.: maghemite (the γ phase) and hematite (the α phase). The phase transition of γ→α-Fe_2O_3 takes place during calcination at about 400 °C [6]. The phase transformation which occurs during calcination gives rise to transformed α-Fe_2O_3 powder which has undergone considerable aggregation and grain growth [7]. The above characteristics are detrimental to the formation of nano-sized α-Fe_2O_3 powder.

Mechanical treatment (mechanochemical reactions) of inorganic solids has become extremely important in many processes in chemical technology, and materials science [8,9]. Many solid state reactions, which normally occur at elevated temperatures, can be facilitated by mechanical treatment [10,11]. In mechanical treatment induced polymorphic transformation, the transition is from a metastable to a stable phase due to the strain energy and shear energy induced by the mechanical treatment.

Mechanochemical effects on the γ→α-Fe_2O_3 phase transformation have been widely discussed in literature. [12,13] The activation energy for the transformation is generally reduced by mechanical treatment applied to γ-Fe_2O_3. However, the effects of mechanical treatment on the morphology of the intermediate and final products and the microstructure development after sintering have not been reported.

The purposes of this study are to use the mechanical activation of γ-Fe_2O_3 to prepare the nano-sized α-Fe_2O_3. and to investigate the mechanical treatment dependence of the phase transformation and sintering of γ-Fe_2O_3 in

* Corresponding author. Tel.: +886-6-2757575x62821; fax: 886-6-2380421.

E-mail address: hsingi@mail.ncku.edu.tw (H.-I. Hsiang).

0272-8842/02/$22.00
PII: S0272-8842(02)00078-0

terms of strain energy using transmission electron microscopy (TEM), X-ray diffractometer (XRD) and scanning electron microscopy (SEM) techniques.

2. Experimental procedure

2.1. Sample preparation

Iron nitrate hydrate (reagent grade) was dissolved in ethanol to prepare Fe^{+3} ethanol solution with concentrations of 0.2 mol/l. A mixture of 0.4 mol/l tartaric acid ethanol solution was prepared. The Fe^{+3} ethanol solution changed abruptly into a viscous sol as soon as tartaric acid solution was added. By heating the sol at 50 °C, ethanol was evaporated off, and a dry iron tartrate powder was obtained. γ-Fe_2O_3 powder was obtained by calcining iron tartrate powder at 300 °C for 2 h. The mechanical treatments were carried out by dry-grinding the γ-Fe_2O_3 powder with a vibration agate mortar and ZrO_2 balls for 1 and 3 h. Both the γ-Fe_2O_3 powders with and without mechanical treatment were calcined at 400 and 500 °C respectively for 2 h, and then compacted by a cold isostatic press at 200 MPa. The green pellet densities determined by dividing the measured mass by the measured volume were approximately 55% of theoretical density (the theoretical density of the γ-Fe_2O_3 powder is 4.89 gm/cm^3). The pellets were sintered at 1200 °C for 2 h.

2.2. Characterization

The crystalline phases in the iron tartrate and calcined powders were identified by the XRD powder method using Ni-filtered CuK_α radiation (D/MAX IIB, Rigaku, Tokyo, Japan), $2\theta = 20$–$60°$. The morphology of the powder was obtained using TEM (200CX, Jeol, Tokyo, Japan) micrograph. The specific surface area was measured using the conventional nitrogen absorption (BET) technique (Gemini 2360, Micromeritics). The microstructure development of the sintered pellet was observed by SEM (S-4100, Hitachi, Tokyo, Japan).

3. Results

3.1. Phase identification

Fig. 1 shows the X-ray diffraction patterns of the gel before and after heat treatment. It can be seen that the phase of the powder calcined at 300 °C was γ-Fe_2O_3. A $\gamma \rightarrow \alpha$-$Fe_2O_3$ phase transformation took place during calcination between 300 and 400 °C. An abrupt increase in the amount of α phase occurred when the calcination temperature rose above 400 °C. α- Fe_2O_3 was the only phase present for the powder calcined above 500 °C.

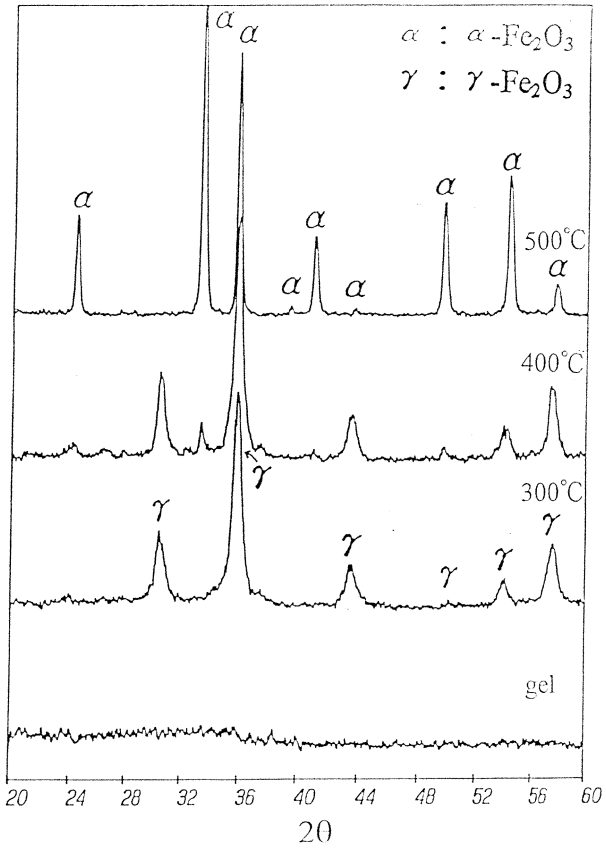

Fig. 1. The X-ray diffraction patterns of the gel before and after heat treatment.

The X-ray diffraction patterns of γ-Fe_2O_3 (obtained by calcination at 300 °C) after various milling times are presented in Fig. 2. It shows no significant change in the XRD patterns before and after milling. After 3 h milling, initially small γ-Fe_2O_3 crystals formed bigger agglomerates (Fig. 3). On the contrary, a relatively weak influence of the milling intensity on the crystallite size was observed.

Fig. 4 shows the X-ray diffraction patterns of γ-Fe_2O_3 powders with various milling time after calcination at 400 °C. γ- and α-Fe_2O_3 co-existed in the unmilled powders. However, only the α-Fe_2O_3 was observed in the milled samples.

3.2. Morphology

Fig. 5 shows the morphology of powders calcined at 300–500 °C. In this figure, fine sub-rounded γ-Fe_2O_3 particles with narrow particle size distribution are observed at 300 °C. At 400 °C, the $\gamma \rightarrow \alpha$-$Fe_2O_3$ phase transformation started and produced a significant alteration in the morphology. The α-Fe_2O_3 formed and coarsened by a chain mechanism [7] induces many neighboring γ crystallites to form one α crystal. At 500 °C, the transformation occurred much more rapidly and resulted in the formation of large colonies of vermicular α-Fe_2O_3.

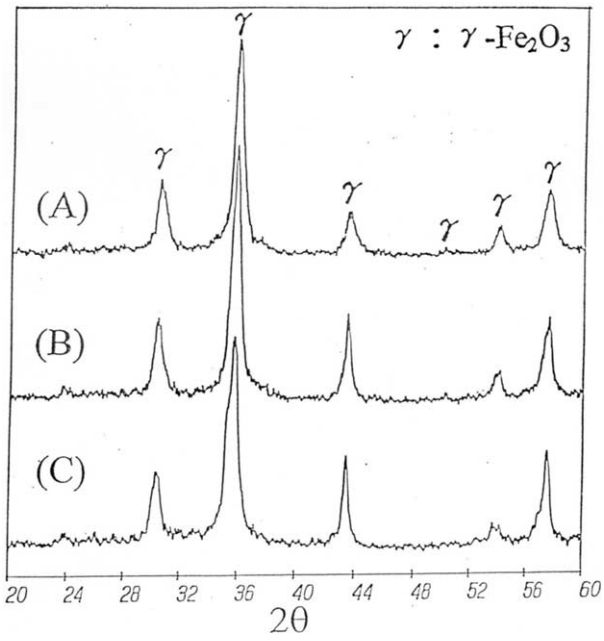

Fig. 2. The X-ray diffraction patterns of γ-Fe_2O_3 (obtained by calcination at 300 °C) (A) without mechanical treatment (B) with 1 h milling(C) with 3 h milling.

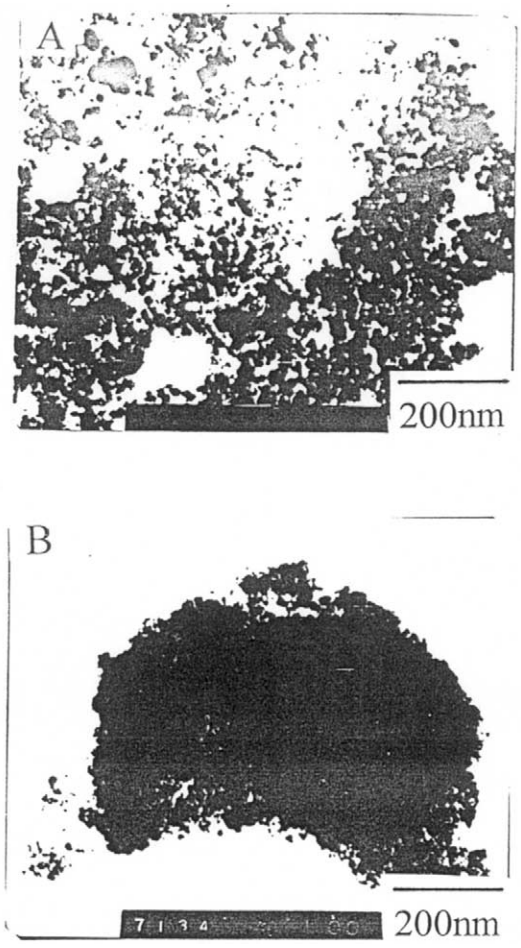

Fig. 3. Transmission electron micrograph of γ-Fe_2O_3 before (A) and after 3 h milling (B).

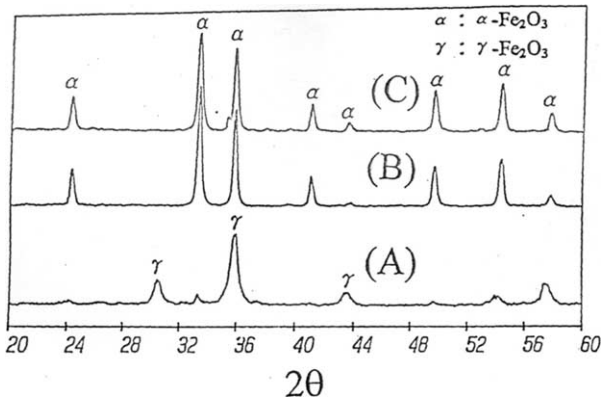

Fig. 4. The X-ray diffraction patterns of γ-Fe_2O_3 powders (A) without mechanical treatment (B) with 1 h milling (C) with 3 h milling after calcination at 400 °C.

The particle morphology of the milled and unmilled samples after calcination at 500 °C are shown in Fig. 6(a) and (b), respectively. α-Fe_2O_3 powder without mechanical treatment become coarsened and aggregated, while the powder with mechanical treatment exhibits very fine equiaxed 50–60 nm particles.

Fig. 7 shows the change in the specific surface area of the milled and unmilled powders at different calcination temperatures. The specific surface area decreased with increasing calcination temperature. Such phenomenon is due to the $\gamma \rightarrow \alpha$-$Fe_2O_3$ phase transformation. At the same temperature, the surface area of the milled powder is larger than that of the unmilled powder because the vermicular microstructure development is inhibited [Fig. 6(b)].

4. Discussion

4.1. Effects of mechanical treatment on $\gamma \rightarrow \alpha$-$Fe_2O_3$ phase transformation

Fig. 4 illustrates that the temperature of $\gamma \rightarrow \alpha$-$Fe_2O_3$ phase transformation for milled powder is lower than that of the powder without mechanical treatment. Zieliński et al. [14] also obtained similar results for Al_2O_3 powder during $\gamma \rightarrow \alpha$-$Al_2O_3$ phase transformation. The temperature of $\gamma \rightarrow \alpha$-$Al_2O_3$ phase transformation decreased with increasing milling time. It was proposed that the decrease in temperature resulted from the presence of internal stress induced by milling in the Al_2O_3 particles. In the present investigation, no broadening of the peaks resulted from lattice strain and crystallite size could be observed after milling (Fig. 2). Solid state phase transformation typically proceeds via nucleation and growth. The interface between two contacting γ-Fe_2O_3 particles can provide the sites for nucleation of α-Fe_2O_3 phase. Thus the nucleation rate is determined by the probability of contact of two γ-Fe_2O_3 particles.

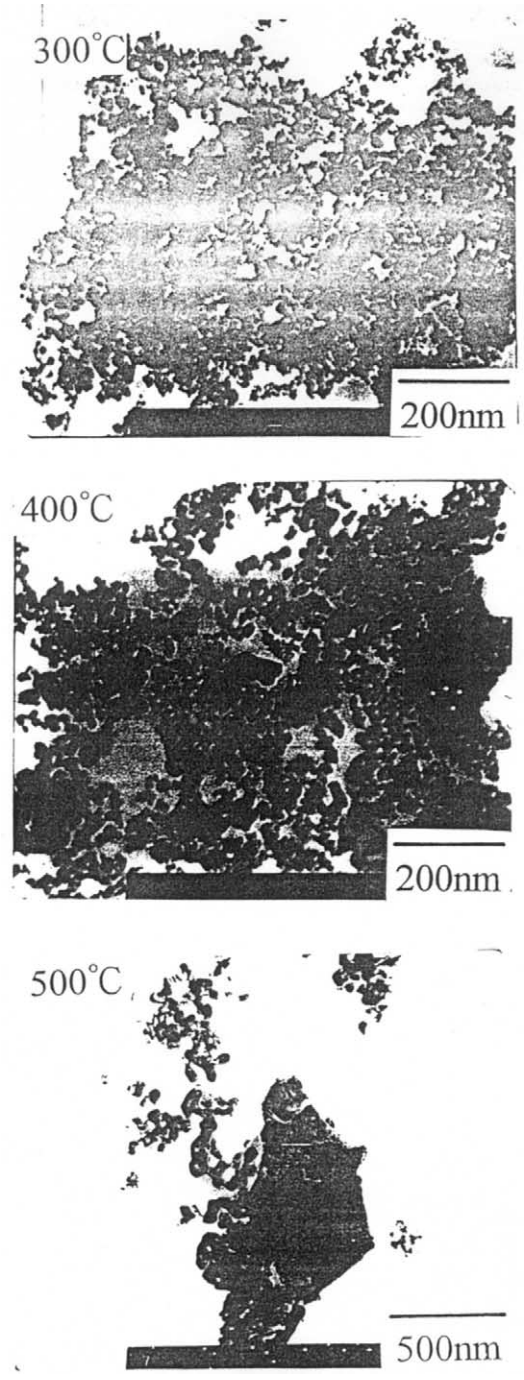

Fig. 5. Transmission electron micrographs of Fe_2O_3 powders calcined at 300, 400 and 500 °C.

Fig. 3 shows that the irregular aggregates of γ-Fe_2O_3 developed after 3 h milling. It may be due to the cold-welding process occurred during milling [15]. Therefore, the γ-Fe_2O_3 particles in the aggregates after milling are expected to have larger average number of surrounding particles in contact with a particle than those without mechanical treatment. Consequently, the temperature of $\gamma \rightarrow \alpha$-$Fe_2O_3$ phase transformation decreased with increasing milling time.

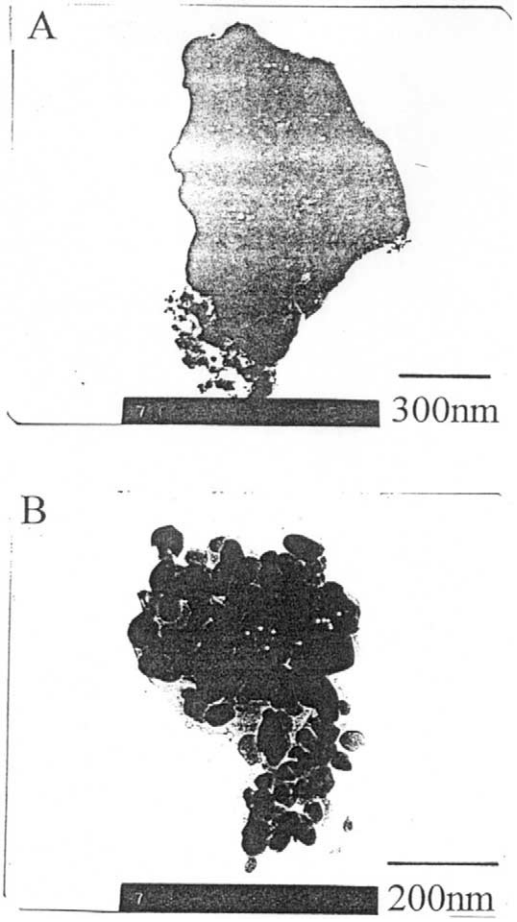

Fig. 6. Transmission electron micrographs of α-Fe_2O_3 powders calcined at 500 °C (A) without mechanical treatment (B) with 3 h milling.

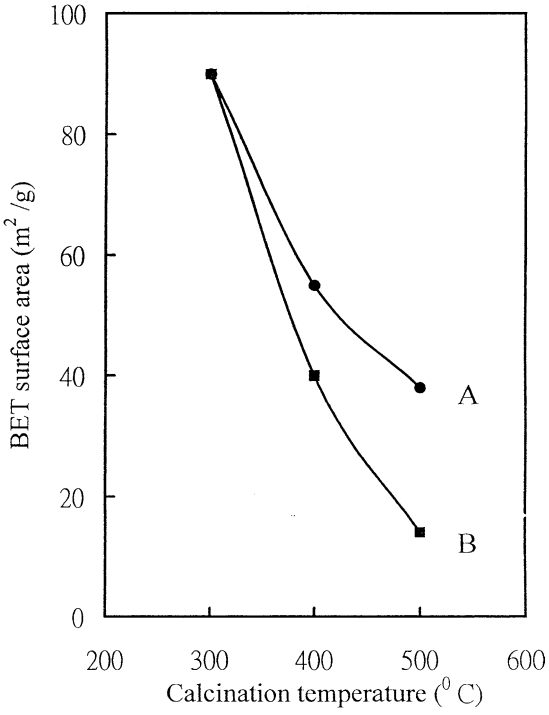

Fig. 7. The change in the specific surface area of the milled (A) and unmilled (B) powders at different calcination temperatures.

4.2. Morphology development

From the above discussion, it is clear that the contact areas associated with the mechanical treatment, having high concentration of defects and lower activation energy barrier for nucleation, can act as nucleation sites. Therefore, a large number of nucleation sites in the milled powder begin growing at approximately the same time during calcination. The high nucleation frequency in the milled powder ensures that the propagation of transformation fronts is arrested by closely spaced adjacent transformation regions and results in the formation of very fine equiaxed particles [Fig. 6 (b)]. Conversely, the unmilled powder has a much smaller nucleation frequency and the nucleation sites do not all nucleate and grow at the same time, thus resulting in a very broad particle size distribution [Fig. 6(a)]. Therefore, mechanical treatment appears to be a good process to obtain nano-sized α-Fe_2O_3 powders.

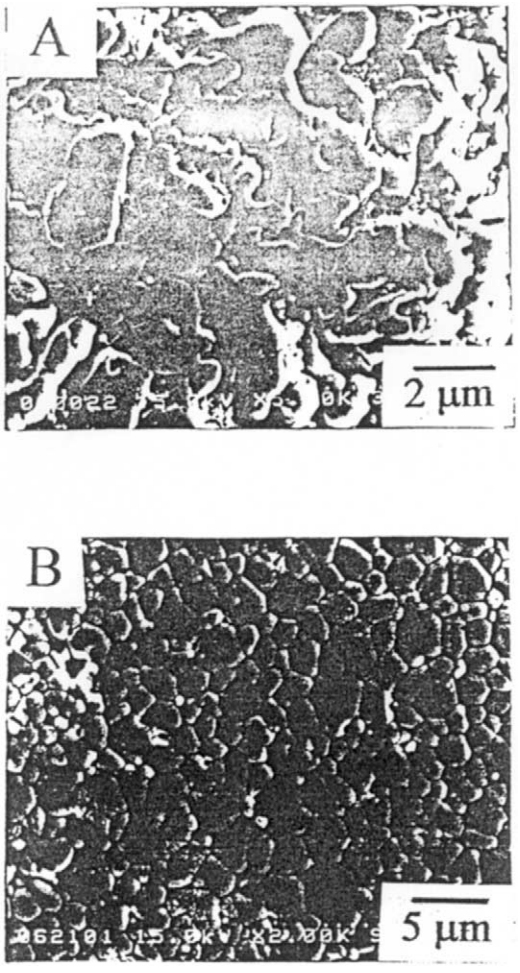

Fig. 8. Microstructure development of α-Fe_2O_3 sintered at 1200 °C (A) without mechanical treatment (B) with 3 h milling.

4.3. Densification

The final microstructures in Fig. 8 show the samples with mechanical treatment for 3 h compared with unmilled samples after sintering at 1200 °C. Clearly the milled sample is highly dense and the unmilled sample is characterized by coarse grains with rather large pores. From the above discussion, it is clear that the mechanical treatment enhances the phase transformation and sintering of γ-Fe_2O_3. The excellent densification behavior of the milled samples is a result of the uniform, fine-grained microstructure that is developed during transformation. Microstructural control is developed through the mechanical treatment of γ-Fe_2O_3 to increase the amount of α-Fe_2O_3 nuclei formed during the $\gamma \rightarrow \alpha$-$Fe_2O_3$ phase transformation and to prevent vermicular microstructure development as a result of α-Fe_2O_3 growth front impingement from adjacent nuclei. However, the large pores and coarse grains found in the unmilled samples were attributed to the development of a coarse, vermicular pore structure during transformation to α-Fe_2O_3.

5. Conclusion

1. Mechanical treatment increased the number of particle contacts, which acted as nucleation sites for the $\gamma \rightarrow \alpha$-$Fe_2O_3$ phase transformation and resulted in lowering the transformation temperature.
2. Mechanical treatment of γ-Fe_2O_3 powders could be an attractive method for the production of nano-sized and equiaxed α-Fe_2O_3 powders.
3. The mechanical treatment of γ-Fe_2O_3 powder enhanced microstructure development by preventing the development of vermicular pore structure during transformation, thus obtaining uniform, fine-grained microstructures after sintering at 1200 °C.

References

[1] R.M. Cornell, U. Schwertmann, The Iron Oxides: Structure, Properties, Reactions, Occurrence and Uses, VCH Publisher, New York, 1996.
[2] W. Zhong, W. Ding, N. Zhang, J. Hong, Q. Yan, Y. Du, Key step in synthesis of ultrafine $BaFe_{12}O_{,19}$ by sol–gel technique, J. Magn. Magn. Mater. 168 (1997) 196–202.
[3] O. Tan, W. Zhu, Q. Yau, L.B. Kong, Size effect and gas sensing characteristics of nanocrystalline x-SnO_2–$(1-x)\alpha$-Fe_2O_3 ethanol sensors, Sensors and Actuators B-Chemical 65 (2000) 361–365.
[4] J.M. Yang, W.J. Tsuo, F.S. Yen, Preparation of ultrafine nickel ferrite powders using mixed Ni and Fe tartrates, J. Sol. Stat. Chem. 145 (1999) 50–57.

[5] K.S. Rane, A.K. Nikumbh, A.J. Mukhedkar, Thermal decomposition of ferrous oxalate dihydrate studied by direct current electrical conductivity measurements, J. Mater. Sci. 16 (1981) 2387–2397.
[6] J. Morales, J.L. Tirado, C. Valera, Preferential X-ray line broadening and thermal behavior of γ-Fe_2O_3, J. Am. Ceram. Soc. 72 (1989) 1244–1246.
[7] W. Feitknecht, U. Mannweiler, Der Mechanismus der Umwandlung von γ-α-Eisen-sesquioxid, Helv. Chim. Acta. 50 (1967) 570.
[8] I.J. Lin, S. Nadiv, Review of the phase transformation and synthesis of inorganic solids obtained by mechanical treatment (mechanomechanical reaction), Mater. Sci. Eng. 39 (1979) 193.
[9] R. Roy, Accelerating the kinetic of low-temperature inorganic syntheses, J. Solid State Chem. 111 (1994) 11.
[10] Y. Nakatani, M. Sakai, S. Nakatani, M. Matsuoka, Mechanochemical effect of dry-grinding on the transformation phenomenon from γ-Fe_2O_3 to α-Fe_2O_3, J. Mater. Sci. Lett. 2 (1983) 129.
[11] E. Mendelovici, A. Sagarzazu, R. Villalba, Processings of iron oxides at room temperature: II. Mechanochemical reaction effects on the structure and surface of pure, synthetic lepidocrocite, Mater. Res. Bull. 17 (1982) 1017–1023.
[12] M. Senna, H. Kuno, Effect of preliminary pressing on isothermal transformation of maghemite to hematite, J. Am. Ceram. Soc. 56 (1973) 492.
[13] H. Imai, M. Senna, Energy storage and liberation of vibro-milled γ-Fe_2O_3, J. Appl. Phys. 49 (1978) 4433–4437.
[14] P.A. Zielinski, R. Schulz, S. Kaliaguine, A. Van Neste, Structural transformations of alumina by high energy ball milling, J. Mater. Res. 8 (1993) 2985.
[15] C. Real, J.M. Criado, V. Balek, Use of emnation thermal analysis in characterization of the influence of grinding on textural and structural properties of nanosized titania powders, J. Mater. Sci. 33 (1998) 5247–5254.